MIT Libraries | DSpace@MIT

MIT Open Access Articles

Non-Invasive Sorting of Lipid Producing Microalgae With Dielectrophoresis Using Microelectrodes

The MIT Faculty has made this article openly available. ***Please share*** how this access benefits you. Your story matters.

Citation: Schor, Alisha R., and Cullen R. Buie. "Non-Invasive Sorting of Lipid Producing Microalgae With Dielectrophoresis Using Microelectrodes." Volume 9: Micro- and Nano-Systems Engineering and Packaging, Parts A and B (November 9, 2012).

As Published: http://dx.doi.org/10.1115/IMECE2012-88317

Publisher: ASME International

Persistent URL: http://hdl.handle.net/1721.1/119176

Version: Final published version: final published article, as it appeared in a journal, conference proceedings, or other formally published context

Terms of Use: Article is made available in accordance with the publisher's policy and may be subject to US copyright law. Please refer to the publisher's site for terms of use.

Massachusetts Institute of Technology

Proceedings of the ASME 2012 International Mechanical Engineering Congress & Exposition
IMECE2012
November 9-15, 2012, Houston, Texas, USA

IMECE2012-88317

NON-INVASIVE SORTING OF LIPID PRODUCING MICROALGAE WITH DIELECTROPHORESIS USING MICROELECTRODES

Alisha R. Schor
Department of Mechanical Engineering
Massachusetts Institute of Technology
Cambridge, Massachusetts, 02139
Email: ducktape@mit.edu

Cullen R. Buie*
Department of Mechanical Engineering
Massachusetts Institute of Technology
Cambridge, Massachusetts, 02139
Email: crb@mit.edu

ABSTRACT

In order to advance the algae biofuel industry, we are constructing a dielectrophoretic, single-cell sorter that selects algae based on lipid content. This tool can lower production costs by aiding in strain selection, online culture monitoring, or directed evolution studies. Dielectrophoresis (DEP) is the polarization of particles or cells in a non-uniform electric field, which leads to a Coulomb force on the cell. Lipids and cell cytoplasm have vastly different dielectric properties. Therefore, as a cell accumulates lipid, we predict a change in the overall DEP response. Our models show that in algae culture medium, we should be able to distinguish between high and low lipid content cells at frequencies above 100 MHz. This was confirmed by experiments, in which high and low lipid cultures of *Neochloris oleoabundans* have DEP crossover frequencies of 190 MHz and 125 MHz, respectively. We have also fabricated a proof-of-concept device validating that cells can be manipulated under DEP. However, in order to achieve sorting, we will require higher frequencies as well as a modified design to eliminate non-uniformities in the electric field through the channel height.

NOMENCLATURE

a Particle radius
E Electric field
ε_i Real permittivity of layer i [F/m]
σ_i Real conductivity of layer i [S/m]
$\tilde{\varepsilon}_i$ Complex permitvity of layer i [F/m]
κ Clausius-Mossotti factor
$\mathbf{F_{DEP}}$ Dielectrophoretic force, time averaged [N]

INTRODUCTION

The commercial use of algae as a biodiesel feedstock is quickly nearing reality. Pilot-scale production facilities have successfully demonstrated the production of biodiesel from microalgae with performance comparable to petrodiesel [1]. In addition, microalgae cultures have been supported on municipal [2] and agricultural [3] wastewater, and many propose CO_2 fixation as another possibility [4, 5].

Scaling these early results to meaningful production levels is currently limited by cost. One mole of algal oil (lipid) yields one mole of biodiesel in the transestherification process. Therefore, any increase in the percentage of lipid contained in individual cells directly increases the volume of biodiesel produced. Naturally, finding or engineering higher lipid content algae will dramatically reduce the price of algal oil per barrel.

However, a high throughput and non-invasive method for sorting single cells based on lipid content does not currently exist. Established methods such as gas chromatography or gravimetric measurement destroy the cells and require large sample volumes [6]. Flow cytometry is a promising and high throughput method, but requires fluorescence staining. Additionally, stains for neutral lipids are limited and not necessarily quantitative [7]. Recent research has shown the lipids can be detected by Raman

*Address all correspondence to this author.

Copyright © 2012 by ASME

Downloaded From: http://proceedings.asmedigitalcollection.asme.org on 10/30/2018 Terms of Use: http://www.asme.org/about-asme/terms-of-use

scattering [8] or nuclear magnetic resonance (NMR) [9], but neither of these includes intrinsic sorting.

To fulfill this need, we have developed a microfluidic device that utilizes dielectrophoresis (DEP) to sort live algae cells based on lipid content. DEP occurs when a non-uniform electric field polarizes a particle and the surrounding media, resulting in a force on the particle. The force is based on the frequency-dependent, complex dielectric properties of the particle itself. This makes DEP highly tunable, since it requires no labeling. All of these factors together make microfluidic DEP an excellent fit for single cell sorting.

THEORY

Dielectrophoresis (DEP) occurs when a particle is polarized by an external non-uniform, electric field. The magnitude and direction of the resulting force is dependent on the size of the particle as well as the complex permittivity of the particle and surrounding medium. Complex permittivity ($\tilde{\varepsilon}$) is, in turn, a function of real permittivity and conductivity, as well as frequency:

$$\tilde{\varepsilon}(\omega) = \sigma - i\frac{\varepsilon}{\omega} \tag{1}$$

The polarization of the particle in a field can be derived by solving Laplace's equation for the electric potential ($\nabla^2\Phi = 0$) inside the particle. For geometries other than spheres and ellipsoids, this derivation is quite complicated, but for spherical particles, the solution to Laplace's equation can be expressed using Legendre polynomials. Knowing the electric field inside the particle allows us to write an effective dipole moment, $\mathbf{p}$. With the dipole moment and the external electric field known, we can calculate the force on the particle using the known expression for electric field force on a dipole, $\mathbf{F} = (\mathbf{p}\cdot\nabla)\mathbf{E}$. The resulting expressions are given below.

$$\mathbf{p} = 4\pi\varepsilon_1 a^3(\kappa)\mathbf{E} \tag{2}$$

$$\mathbf{F_{DEP}} = 2\pi a^3 \varepsilon_1 \mathrm{Re}(\kappa)\nabla|\mathbf{E}_{rms}|^2 \tag{3}$$

$$\kappa(\omega) = \frac{\tilde{\varepsilon}_2 - \tilde{\varepsilon}_1}{\tilde{\varepsilon}_2 + 2\tilde{\varepsilon}_1} \tag{4}$$

where $\kappa(\omega)$ is the Clausius-Mossotti factor, a is the particle radius, ε_1 is the absolute, real permittivity of the surrounding medium, and $\mathbf{E}$ is the electric field. The subscripts 1 and 2 for complex permittivities refer to the medium and the cell, respectively. Equation 3 is a time-averaged value for a sinusoidally applied electric field at frequency ω.

Other models have been derived for particles with inhomogeneous complex permittivities. In particular, effective polarizabilities for multi-shelled spheres are quite common and are good representations of living cells or organisms [10–12]. In our work, we model a single algal cell as a double-shelled sphere (Fig. 1). The outer shell is thin and represents the cell membrane. The innermost body represents the lipids within the cell. The remaining, intermediate layer describes the cytoplasm.

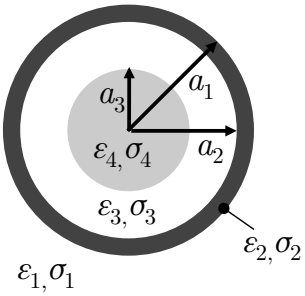

FIGURE 1. A SINGLE ALGAE CELL HAS AN EFFECTIVE POLARIZABILITY DESCRIBED BY THE DOUBLE SHELL MODEL DERIVED BY [13]. REGION ONE REPRESENTS THE SURROUNDING MEDIUM. REGIONS TWO, THREE AND FOUR REPRESENT THE CELL MEMBRANE, CYTOPLASM AND LIPID BODY, RESPECTIVELY.

For the double-shell model given in Fig. 1, the Clausius-Mossotti factor is

$$\kappa_{dbl} = \frac{\tilde{\varepsilon}_{34} - \tilde{\varepsilon}_1}{\tilde{\varepsilon}_{34} + 2\tilde{\varepsilon}_1}, \tag{5}$$

with

$$\tilde{\varepsilon}_{34} = \tilde{\varepsilon}_2 \frac{g_{23}^3 + 2\frac{\tilde{\varepsilon}_{23} - \tilde{\varepsilon}_2}{\tilde{\varepsilon}_{23} + 2\tilde{\varepsilon}_2}}{g_{23}^3 - \frac{\tilde{\varepsilon}_{23} - \tilde{\varepsilon}_2}{\tilde{\varepsilon}_{23} + 2\tilde{\varepsilon}_2}} \tag{6}$$

$$\tilde{\varepsilon}_{23} = \tilde{\varepsilon}_2 \frac{g_{12}^3 + 2\frac{\tilde{\varepsilon}_3 - \tilde{\varepsilon}_2}{\tilde{\varepsilon}_3 + 2\tilde{\varepsilon}_2}}{g_{12}^3 - \frac{\tilde{\varepsilon}_3 - \tilde{\varepsilon}_2}{\tilde{\varepsilon}_3 + 2\tilde{\varepsilon}_2}}, \tag{7}$$

$$g_{12} = a_1/a_2 \tag{8}$$

$$g_{23} = a_2/a_3 \tag{9}$$

The frequency dependence has been omitted for clarity but is implied in all complex values. The subscripts are again numbered from the medium inward, such that layers 1, 2, 3 and 4 represent the medium, membrane, cytoplasm, and internal lipid body, respectively.

Copyright © 2012 by ASME

Downloaded From: http://proceedings.asmedigitalcollection.asme.org on 10/30/2018 Terms of Use: http://www.asme.org/about-asme/terms-of-use

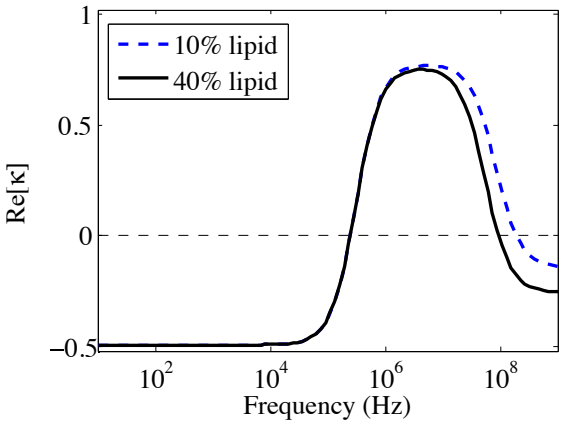

FIGURE 2. THE CLAUSIUS-MOSSOTTI FACTOR AS A FUNCTION OF FREQUENCIES FOR MODEL CELLS CONTAINING 10% (SOLID) AND 40% (DASHED) LIPIDS BY VOLUME. A DOUBLE-SHELLED MODEL [13] WAS USED TO DETERMINE κ.

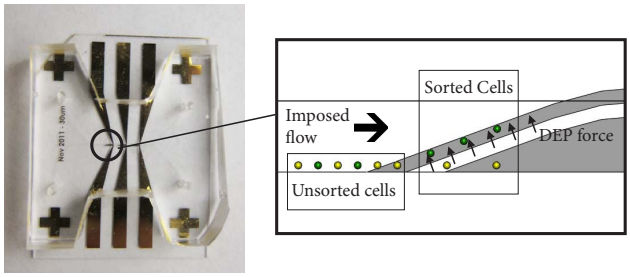

FIGURE 3. CELLS ARE DRIVEN LONGITUDINALLY DOWN A MICROCHANNEL IN OUR DEVICE. EMBEDDED ELECTRODES CREATE AREAS OF STEEP ELECTRIC FIELD GRADIENT AT THE ELECTRODE EDGES. AS CELLS PASS OVER THIS REGION, CELLS OF INTEREST ARE DEFLECTED LATERALLY ACROSS THE CHANNEL INTO AN ALTERNATIVE OUTLET.

DESIGN

Cell Sorting

As previously stated, Equation 3 shows the dependence of the DEP force on particle size, frequency, complex permittivity and field geometry. Sorting by DEP therefore relies on exploiting differences in one of these properties to impart distinct forces on individual particles. Inspecting the Clausis-Mossotti factor (Eq. 4), we can see that the direction of the DEP force changes depending on whether the complex particle or medium permittivity is greater (at a given frequency). Positive DEP (pDEP) the particle permittivity is greater and results in forces directed *toward* regions of highest electric field gradient. When the medium permittivity is higher, negative DEP (nDEP) acts *away* from regions of high electric field gradient.

In order to sort high- and low-lipid-content cells, we design the electric field and choose the input frequency such that the DEP force acting on each subpopulation is different. We hypothesize that as cells accumulate lipids, their complex permittivity drops, since lipids have significantly lower permittivity *and* conductivity than cytoplasm [14, 15]. Using representative values from literature, we can plot κ over a range of frequencies. Figure 2 shows theoretical spectra for cells containing 10% and 40% lipids. The figure shows that at a frequency of 220 MHz, the high lipid cell will experience nDEP while the low lipid cell experiences pDEP.

Our device utilizes nDEP, specifically, to deflect selected particles across a microchannel and into one of two outlets. Unwanted (low-lipid) particles experience no DEP force and pass over the selection zone, unaffected, into the second outlet. The microfluidic device is shown in Fig. 3. The inlet of the device consists of a particle inlet as well as a focusing stream that directs particles toward the "default" outlet. Microelectrodes embedded at the bottom of the channel create an asymmetric field that is angled toward the second outlet. At the appropriate frequency, high-lipid-content cells experience nDEP as they pass over these electrodes and are directed to the second outlet.

Device configuration

Electrode geometry is a crucial element in designing our device. The electrodes must impose an electric field that is strong enough to overcome the drag force of the incoming flow and be positioned so that the particles are directed toward the correct outlet. A somewhat unique aspect to this design problem is that it is not the actual *shape* of the electric field that we are interested in, but the shape of the *gradient*.

Beginning with a nominal channel width of 100 μm and requiring that the cell be transported across the channel in less than one second, our transverse velocity is 1×10^{-4} m/s (Reynolds number $\approx 10^{-4}$). Stokes' drag force on a spherical particle is given as $6\pi\mu a\mathbf{v}$, and is approximately 2.0 pN at this velocity. Therefore, our electrode geometry must produce a DEP force that is at least 2.0 pN. Referring to Eq. 3, this in turn requires an electric field gradient on the order of 10^{14} V^2/m^3. Using COMSOL, we simulated the electric field in our device (Fig. 4). The average transverse gradient (perpendicular to the flow) is approximately 10^{15} V^2/m^3, which is more than sufficient to move the cells. The angle and length of the electrodes are somewhat arbitrary, but are intended to maximize the residence time of the cell in the field. Figure 4 shows the magnitude of the electric field ($|E|^2$) around the electrodes and the simulated trajectories of high lipid cells in the device.

Copyright © 2012 by ASME
Downloaded From: http://proceedings.asmedigitalcollection.asme.org on 10/30/2018 Terms of Use: http://www.asme.org/about-asme/terms-of-use

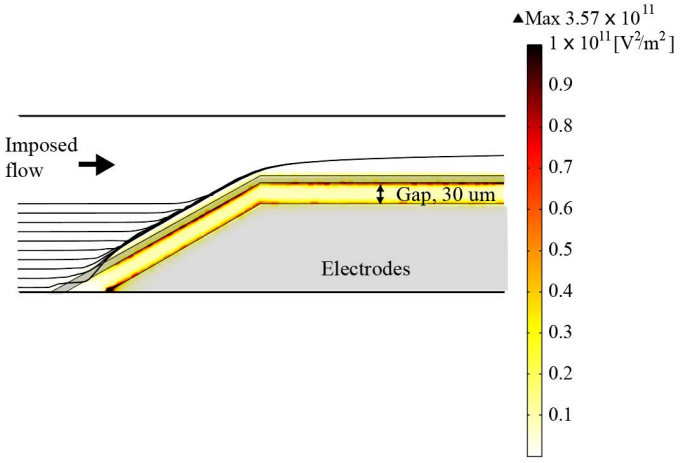

FIGURE 4. BLACK LINES SHOW SIMULATED TRAJECTORIES OF HIGH LIPID ALGAE FLOWING OVER THE ELECTRODES, SHADED GRAY. THE COLORBAR INDICATES THE MAGNITUDE OF THE ELECTRIC FIELD, SQUARED ($|E|^2$). A NEGATIVE DEP FORCE DEFLECTS CELLS AROUND THE ELECTRODE GAP.

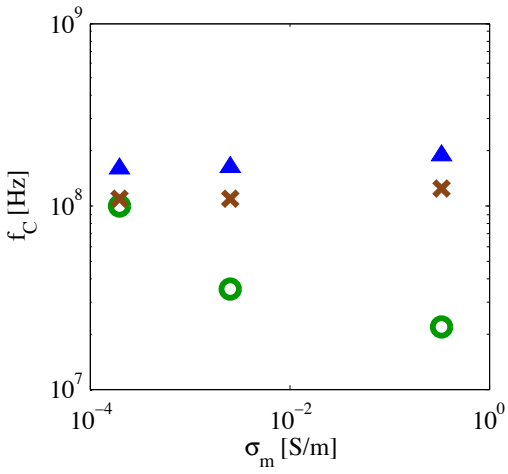

FIGURE 5. CROSSOVER FREQUENCIES FOR THREE CULTURES IN THREE MEDIUM CONDUCTIVITIES. *N. OLEOABUNDANS* GROWN WITH NITROGEN (BLUE TRIANGLES) AND WITHOUT NITROGEN (BROWN CROSSES) HAVE DISTINCT CROSSOVER FREQUENCIES. A THIRD CULTURE OF *C. REINHARDTII* (GREEN CIRCLES) IS IDENTIFIABLE BY ITS CROSSOVER FREQUENCY AS WELL.

MATERIALS AND METHODS

Microfabrication

The microchannels were formed by standard polydimethylsiloxane (PDMS) soft-lithography techniques: A silicon master was created by spin-coating a 30 µm layer of SU-8 onto a blank silicon wafer. The channel geometry was defined using a negative photomask and the unexposed SU-8 was washed away. PDMS (Dow-Corning) was poured onto the master in a ratio of 10:1 (base:curing agent) and the wafers were baked for 2 hours at 80°C. Individual devices were then cut apart and access ports were punched using biopsy punches.

Electrodes were deposited onto glass coverslips using electron beam evaporation. AZ5214 (Clariant) photoresist was used to define the electrode geometry. A 15nm titanium adhesion layer was plated prior to 150 nm of gold. Following metal evaporation, the remaining photoresist was dissolved using RR4 resist developer. The coverslips were adhered to the PDMS to form closed channels using a Harrick Plasma Cleaner.

Hardware

The electric field was generated using a high-frequency function generator (Tabor Electronics). Wires were soldered to gold, spring-loaded contacts to make connections to the leads plated on each coverslip. The signal from the function generator was applied directly to the wires. Measuring DEP response was performed using the brightfield of an inverted microscope (Nikon).

Cell Culture

Algal cultures were purchase from The Culture Collection of Algae at the Univeristy of Texas at Austin. *Neochloris oleoabundans* (1185) and *Chlamydomonas reinhardtii* (LB2607) were maintained in liquid culture in Modifield Bold 3N Medium. Cultures were kept on a 12h/12h light and dark cycle using a fluorescent lamp and perfused with dry air supplemented with 1.5% CO_2.

RESULTS

Cells grown in our laboratory were first characterized based on the dielectrophoretic response. We measured three cultures: *C. reinhardtii* under normal growth conditions, *N. oleoabundans* under normal growth conditions, and *N. oleabundans* starved of nitrogen, which is known to cause lipid accumulation. For each of these cultures, we recorded their dielectrophoretic response (zero, positive or negative) over a range of frequencies and in three different medium conductivities. This allowed us to find the crossover frequency, f_c, i.e. the frequency of no DEP force. These findings are shown in Fig. 5. Only the higher of the two predicted crossover frequencies were recorded.

Each of the three cultures showed a distinct crossover frequency at all medium conductivities. Notably, the crossover frequencies of *N. oleoabundans* grown with and without nitrogen were separated by at least 50 MHz in all cases. Nitrogen starvation is known to cause cells to accumulate significant fractions

Copyright © 2012 by ASME
Downloaded From: http://proceedings.asmedigitalcollection.asme.org on 10/30/2018 Terms of Use: http://www.asme.org/about-asme/terms-of-use

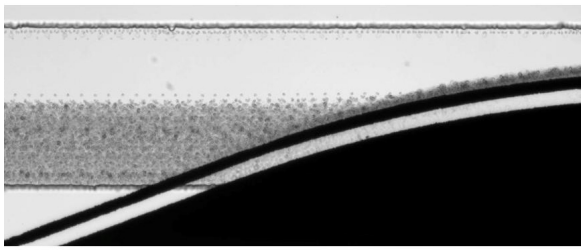

FIGURE 6. EXAMPLE OF LIVE ALGAE CELLS DEFLECTED AROUND AN ELECTRODE GAP UNDER THE INFLUENCE OF NEGATIVE DEP. AN INPUT SIGNAL OF 20 V_{PP}, 5 MHZ WAS USED IN THIS EXPERIMENT.

of neutral lipids in many algae species [16–18]. As noted above, our device separates cells by operating at a frequency at which the cells of interest experience nDEP while other cells experience no force. Figure 5 shows that in 0.3 S/m medium[1], high-lipid-content (nitrogen starved) cells will go from positive to negative DEP at 125 MHz, while low-lipid-content cells do not transition until 190 MHz. Therefore, operating our device at frequencies between these two crossovers will sort high- and low-lipid cells. The even more distinct electrical signature of *C. reinhardtii* is likely a result of its having a significantly different structure.

We were also able to manipulate live algae cells in our device. This is shown in a time-lapse image (Fig. 6) for *C. reinhardtii* cells. The electrodes were charged with a 20 V_{pp}, 5 MHz signal. Nearly all of the cells are deflected around the gap, as predicted. Some cells are deflected upward through the channel—out of plane—and can be seen as out-of-focus shadows in the gap. By operating at higher frequencies, we were also able to induce pDEP, in which cells trap at the electrode edges (results not shown). Increasing the frequency further, we transition back to nDEP, with the high-lipid cells experiencing this transition first (see Fig. 5). We have validated this effect in early experiments, but the results are still being evaluated.

DISCUSSION

As a first step toward validating our model, we have determined the crossover frequencies of our cultures in various mediums. This will also help us choose our device operating frequency. The crossover frequencies shown in Fig. 5 are in the expected range for a spherical, two-shelled cell based on previously reported electrical properties. The lower crossover frequencies (results not shown) also qualitatively match.

Ultimately, we would like to construct Clausius-Mossotti factor spectra for our cells in particular, rather than using nominal values from literature. One way to do this is to measure the velocity at which a cell moves under dielectrophoresis. For small particles, inertia is negligible and the DEP force is exactly balanced by Stokes' drag. By measuring velocity, then, we can determine the magnitude of the force. Then, by dividing out all of the coefficients in Eq. 3, we can calculate the real part of the Clausius-Mossotti factor. Similar experiments have been done by measuring the threshold velocity of a DEP trap [19–21].

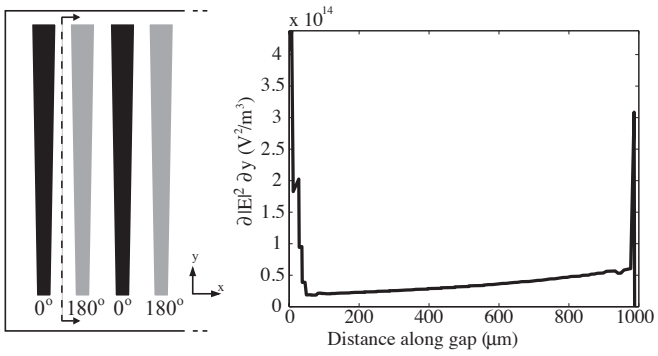

FIGURE 7. PROPOSED ELECTRODE GEOMETRY FOR CALCULATING $\kappa(\omega)$. CELL VELOCITIES MEASURED FROM VIDEOS YIELD THE MAGNITUDE OF THE DEP FORCE. COMBINING THIS WITH THE KNOWN, LINEAR ELECTRIC FIELD GRADIENT (RIGHT) ALLOWS US TO CALCULATE κ. THE FIELD SHOWN IS TIME-AVERAGE FOR A 10 V_{PP} SIGNAL.

A proposed electrode geometry for this experiment is given in Figure 7. These tapered, interdigated electrodes were used in [22] to sort cells based on their dielectrophoretic equilibrium point across the width of the channel. The advantage of this shape for our purposes is that it generates an electric field gradient that varies linearly in the y-direction (Fig. 7, right), which greatly simplifies the calculations to determine $\kappa(\omega)$. (Spikes in the gradient do occur at the electrode edges due to fringe fields, so measurements from these regions should be excluded.) Alternating electrodes are charged 180° out of phase, and the taper generates a gradient in the gap between and along the length of the electrodes. Cells intitally at rest will move in the y-direction when an electric field is turned on. The velocity of their motion can be used to determine the force acting on it and then the Clausius-Mossotti factor.

We also demonstrated a proof of concept microfluidic device that redirected live algae cells toward a given outlet. This validated the working principle of nDEP as a flow through sorting mechanism. One caveat, however, is that this was done below the first crossover frequency, rather than above the second. In this regime, while we do observe nDEP, sorting is not possible because changes in internal lipid content will not change the Clausius-Mossotti factor. In moving toward sorting of a hetere-

[1]This experiment was performed in cell growth medium, rather than a prepared salt solution.

Copyright © 2012 by ASME

Downloaded From: http://proceedings.asmedigitalcollection.asme.org on 10/30/2018 Terms of Use: http://www.asme.org/about-asme/terms-of-use

ogenous population, we will have to operate in the >100 MHz range, as shown in Figs. 2 and 5. Operating at such high frequencies introduces new practical considerations, as parasitic capacitances (as well as the capacitance of the actual device) will significantly attenuate the signal. Preliminary experiments have confirmed that *N. oleoabundans* cells deflect under negative DEP in this regime. However, we are still developing the circuitry required to operate in this very high frequency (VHF) regime.

CONCLUSION

Early prototypes, along with qualitative characterization of cells grown in house, show promising results. We were able to measure reasonably large changes in crossover frequency between two of the same species grown under different conditions. One of these conditions, nitrogen starvation, is known to cause significant lipid accumulation in this algae [16, 17]. In addition, we showed that our electrode geometry is capable of deflecting live, flowing algae across the channel, away from one outlet and toward another.

There still remains significant work to achieve our goal of binary sorting. First, we will have to operate our device in the 150 MHz frequency range in order to distinguish between high and low lipid cells. This will require additional electronics, since the device impedance is extremely low in this frequency range.

The second major hurdle is the deflection of cells perpendicular to the plane of the electrodes. Using planar electrodes results in an electric field that is non-uniform through the height of the channel. The field decreases in magnitude with increasing height, which causes the upward deflection of cells. In addition to being deflected into a region of lower DEP force, cells are transported to faster-moving streamlines in the center of the channel. Both of these behaviors significantly reduce sorting efficacy. Moving forward, we intend to fabricate devices with electrodes on both the top and bottom of the channels. This will produce an electric field that is non-uniform in-plane only, supporting higher DEP forces and flow rates.

PAPER NUMBER

IMECE2012-88317

ACKNOWLEDGMENT

The authors would like to thank Dr. Korneel Rabaey for discussion, as well as a collaboration under the DuPont-MIT alliance. They also acknowledge the facilities at the Microsystems Technology Laboratory (MTL) at MIT where fabrication for this project took place.

REFERENCES

[1] Rodolfi, L., Zittelli, G. C., Bassi, N., Padovani, G., Biondi, N., Bonini, G., and Tredici, M. R., 2009. "Microalgae for oil: Strain selection, induction of lipid synthesis and outdoor mass cultivation in a low-cost photobioreactor". *Biotechnology and Bioengineering,* ***102***, pp. 100 –112.

[2] Mutanda, T., Karthikeyan, S., and Bux, F., 2011. "The utilization of post-chlorinated municipal domestic wastewater for biomass and lipid production by *Chlorella* spp. under batch conditions". *Applied Biochemistry and Biotechnology*, pp. 1–13. 10.1007/s12010-011-9199-x.

[3] Pittman, J. K., Dean, A. P., and Osundeko, O., 2011. "The potential of sustainable algal biofuel production using wastewater resources". *Bioresource Technology,* ***102***(1), pp. 17 – 25. Special Issue: Biofuels - II: Algal Biofuels and Microbial Fuel Cells.

[4] Kumar, A., Ergas, S., Yuan, X., Sahu, A., Zhang, Q., Dewulf, J., Malcata, F. X., and van Langenhove, H., 2010. "Enhanced CO_2 fixation and biofuel production via microalgae: recent developments and future directions". *Trends in Biotechnology,* ***28***(7), pp. 371 – 380.

[5] Powell, E., and Hill, G., 2010. "Carbon dioxide neutral, integrated biofuel facility". *Energy,* ***35***, pp. 4582–4586.

[6] James, G. O., Hocart, C. H., Hillier, W., Chen, H., Kordbacheh, F., Price, G. D., and Djordjevic, M. A., 2011. "Fatty acid profiling of *Chlamydomonas reinhardtii* under nitrogen deprivation". *Bioresource Technology,* ***102***(3), pp. 3343 – 3351.

[7] Chen, W., Sommerfeld, M., and Hu, Q., 2011. "Microwave-assisted Nile red method for in vivo quantification of neutral lipids in microalgae". *Bioresource Technology,* ***102***(1), pp. 135 – 141.

[8] Huang, Y., Beal, C., Cai, W., Ruoff, R., and Terentjev, E., 2010. "Micro-raman spectroscopy of algae: Composition analysis and fluorescence background behavior". *Biotechnology and Bioengineering,* ***105***(5), pp. 889–898.

[9] Beal, C., Webber, M., Ruoff, R., and Hebner, R., 2010. "Lipid analysis of neochloris oleoabundans by liquid state NMR". *Biotechnology and Bioengineering,* ***106***(4), pp. 573–583.

[10] Asami, K., 2002. "Characterization of biological cells by dielectric spectroscopy". *Journal of Non-Crystalline Solids,* ***305***(1-3), pp. 268 – 277.

[11] Broche, L. M., Labeed, F. H., and Hughes, M. P., 2005. "Extraction of dielectric properties of multiple populations from dielectrophoretic collection spectrum data". *Physics in Medicine and Biology,* ***50***, pp. 2267–2274.

[12] Chung, C., Waterfall, M., Pells, S., Menachery, A., Smith, S., and Pethig, R., 2011. "Dielectrophoretic characterisation of mammalian cells above 100 MHz". *Journal of Electrical Bioimpedance,* ***2***, pp. 64–71.

[13] Irimajiri, A., Hanai, T., and Inouye, A., 1979. "A dielectric

Copyright © 2012 by ASME

Downloaded From: http://proceedings.asmedigitalcollection.asme.org on 10/30/2018 Terms of Use: http://www.asme.org/about-asme/terms-of-use

theory of "multi-stratified shell" model with its application to a lymphoma cell". *Journal of Theoretical Biology,* ***78***(2), pp. 251 – 269.

[14] Markx, G. H., and Davey, C. L., 1999. "The dielectric properties of biological cells at radiofrequencies: applications in biotechnology". *Enzyme and Microbial Technology,* ***25***(3-5), pp. 161 – 171.

[15] Malmstadt, N., Nash, M. A., Purnell, R. F., and Schmidt, J. J., 2006. "Automated formation of lipid-bilayer membranes in a microfluidic device". *Nano Letters,* ***6***(9), pp. 1961–1965.

[16] Chisti, Y., 2007. "Biodiesel from microalgae". *Biotechnology Advances,* ***25***(3), pp. 294 – 306.

[17] Griffiths, M., and Harrison, S., 2009. "Lipid productivity as a key characteristic for choosing algal species for biodiesel production". *Journal of Applied Phycology,* ***21***, pp. 493–507.

[18] Gouveia, L., and Oliveira, A., 2009. "Microalgae as a raw material for biofuels production". *Journal of Industrial Microbiology & Biotechnology,* ***36***, pp. 269–274. 10.1007/s10295-008-0495-6.

[19] Li, H., Zheng, Y., Akin, D., and Bashir, R., 2005. "Characterization and modeling of a microfluidic dielectrophoresis filter for biological species". *Microelectromechanical Systems, Journal of,* ***14***(1), Feb, pp. 103 – 112.

[20] Voldman, J., Braff, R. A., Toner, M., Gray, M. L., and Schmidt, M. A., 2001. "Holding forces of single-particle dielectrophoretic traps". *Biophysical Journal,* ***80***(1), pp. 531 – 542.

[21] Zhu, J., Tzeng, T.-R. J., and Xuan, X., 2010. "Continuous dielectrophoretic separation of particles in a spiral microchannel". *Electrophoresis,* ***31***, pp. 1382–1388.

[22] Lin, J., and Yeow, J., 2007. "Enhancing dielectrophoresis effect through novel electrode geometry". *Biomedical Microdevices,* ***9***(6), December, pp. 823–831.

Copyright © 2012 by ASME

Downloaded From: http://proceedings.asmedigitalcollection.asme.org on 10/30/2018 Terms of Use: http://www.asme.org/about-asme/terms-of-use